ROP Inception: Signal Estimation With Quadratic Random Sketching

Remi Delogne*, Vincent Schellekens†, Laurent Jacques*

*: ICTEAM/INMA, UCLouvain, †: CEA List - LFIC, France

1. Problem statement and contribution

An increasing amount of algorithms in signal processing, data science or optimisations rely on random projections (or *sketching*) to alleviate the computational burden of large datasets with dimensionality reduction.

- Target task: estimating specific functions of signals (*e.g.*, signal estimation ≡ similarity with a probing pattern),
- Challenge: How to estimate those functions in a *sketched* domain?
- Applications: Event detection or localised statistics in compressed video streams.

Context of this work:

- Signal acquisition with *quadratic random sketching* [3],
- Motivation: optical processing unit (OPU), an optical sketching in linear time [2] (see Box 2).

Our contribution (see related paper [1]):

- Signal estimation in the sketched domain with bounded error,
- Error controlled by the number of random measurements.

2. Optical processing unit

In an OPU, a laser beam—front coded by an input binary image using a spatial light modulator (see Fig. 1)—propagates through a scattering material. Light scattering physics shows that the scattered light intensity recorded on a camera at the output of the material amounts to quadratic random projections of the coded front, *i.e.*, the image [2]. Moreover, these projections are stable through time, which allows for reproducible sketching, up to some noise. An OPU can thus sketch large images at large sketching dimensions "at the speed of light" and low power consumption.

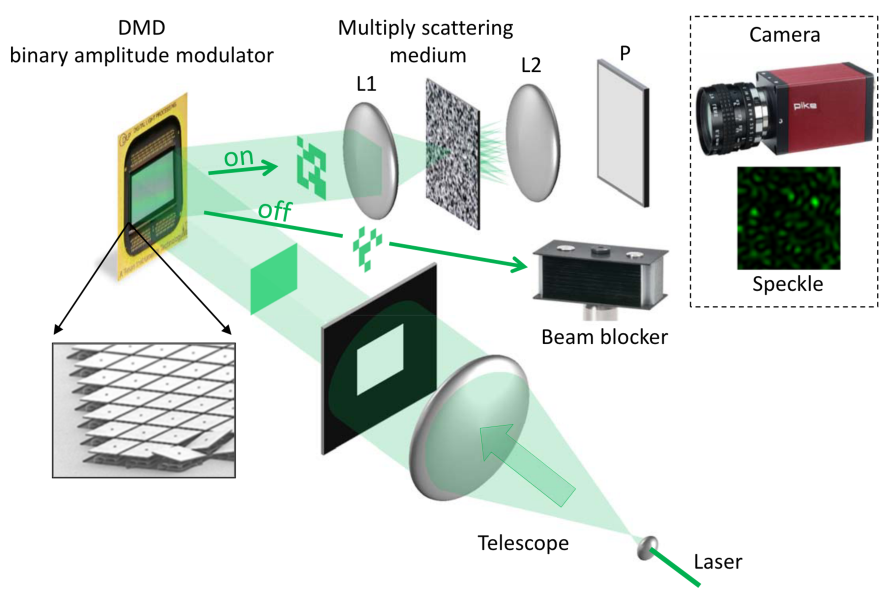

Figure 1: Schematic representation of the OPU process,

3. Mathematical framework

We thus consider a sketching based on random quadratic projections of a vector $\boldsymbol{x} \in \mathbb{R}^n$. It is modeled as follows.

- Given $2m$ Gaussian random vectors $(\boldsymbol{a}_i)_{i=1}^{2m}$, $a_{ij} \sim_{\text{i.i.d.}} \mathcal{N}(0,1)$, define:

$$\mathcal{A}^{\text{v}} : \boldsymbol{x} \in \mathbb{R}^n \mapsto \mathcal{A}^{\text{v}}(\boldsymbol{x}) := \big((\boldsymbol{a}_1^\top \boldsymbol{x})^2, \ldots, (\boldsymbol{a}_{2m}^\top \boldsymbol{x})^2\big)^\top \in \mathbb{R}_+^{2m}. \tag{1}$$

- This non-linear sketch models the OPU action. It is also linear with respect to the *lifted signal*, the rank-one PSD matrix $\boldsymbol{X} = \boldsymbol{x}\boldsymbol{x}^\top$:

$$\mathcal{A}^{\text{v}}(\boldsymbol{x}) = \big((\boldsymbol{a}_i^\top \boldsymbol{x})^2\big)_{i=1}^m = \big(\boldsymbol{a}_i^\top \boldsymbol{x}\boldsymbol{x}^\top \boldsymbol{a}_i\big)_{i=1}^{2m} = \big(\langle \boldsymbol{A}_i, \boldsymbol{X}\rangle\big)_{i=1}^{2m} =: \mathcal{A}(\boldsymbol{X}) \tag{2}$$

- $\mathcal{A}$ is made of rank-one projections (ROP) of $\boldsymbol{X}$; $\mathcal{A}^{\text{v}}$ and $\mathcal{A}$ are in fact non isotropic: their expectations do depend on their input direction.
- The *debiased ROP* $\mathcal{B}$ solves the problem [3]: $\mathbb{E}\mathcal{B}(\boldsymbol{x}) \propto \|\boldsymbol{x}\|^2$ with

$$\boldsymbol{x} \in \mathbb{R}^n \mapsto \mathcal{B}(\boldsymbol{x}) = \big(\mathcal{A}_{2i}^{\text{v}}(\boldsymbol{x}) - \mathcal{A}_{2i+1}^{\text{v}}(\boldsymbol{x})\big)_{i=1}^m \in \mathbb{R}_+^m. \tag{3}$$

- $\mathcal{B}$ is easily implementable from an OPU's output [2].

4. The sign Product Embedding

Performing signal estimation in the sketched domain is supported by the *Sign Product Embedding* (SPE) property of $\mathcal{B}$.

Given a *unit* vector $\boldsymbol{u} \in \mathbb{R}^n$, and a distortion $0 < \delta < 1$, provided that

$$m \gtrsim \delta^{-2} k \log(n/k\delta),$$

then for all k-sparse signals $\boldsymbol{x} \in \mathbb{R}^n$, the following equation holds with probability exceeding $1 - C\exp(-c\delta^2 m)$ (for some $C, c > 0$):

$$\Big| \tfrac{\pi}{4m}\langle \operatorname{sign}(\mathcal{B}(\boldsymbol{u})), \mathcal{B}(\boldsymbol{x})\rangle \;-\; \langle \boldsymbol{u}, \boldsymbol{x}\rangle^2 \Big| \;\leq\; \delta\, \|\boldsymbol{x}\|^2. \tag{4}$$

This means that for m sufficiently large, projecting $\mathcal{B}(\boldsymbol{x})$ onto $\operatorname{sign}(\mathcal{B}(\boldsymbol{u}))$ gives a close approximation of $\langle \boldsymbol{x}, \boldsymbol{u}\rangle^2$, the (squared) similarity between $\boldsymbol{x}$ and $\boldsymbol{u}$.

5. Experiments I (simulations)

Localised occupancy: We analyse a sequence of video frames $\{\boldsymbol{x}_t\}_{t=0}^{23}$, representing a white revolving disk on a dark background. We aim to detect the passage of the disk in single quadrants directly in the sketched domain using normalised restriction vectors over the four quadrants, $\{\boldsymbol{u}_j\}_{j=0}^{3}$ by estimating $\langle \boldsymbol{u}_j, \boldsymbol{x}_t\rangle^2$ with the SPE, *i.e.*, from $\langle \operatorname{sign}(\mathcal{B}(\boldsymbol{u}_j)), \mathcal{B}(\boldsymbol{x}_j)\rangle$.

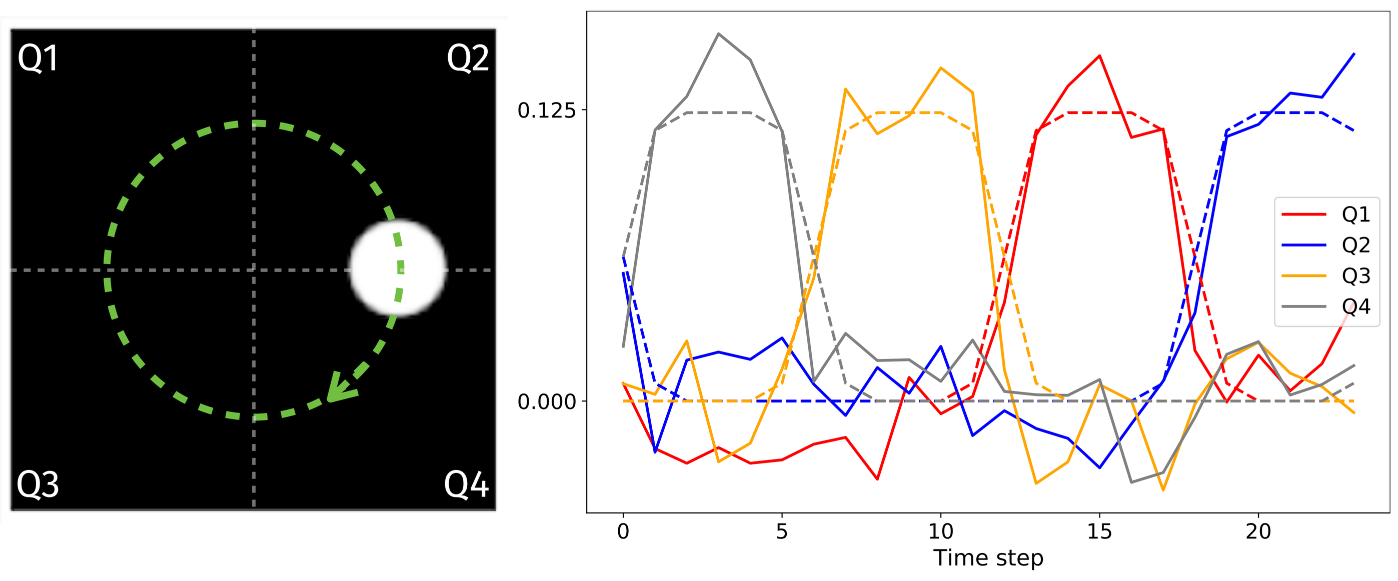

Figure 2: Left: Graphical representation of frame sequence, Right: Estimation of quadrant occupancy functions per quadrant (ground truth in dashed lines).

Classification in the sketched domain: Using hand-written digits (MNIST, 70k images belonging to 10 classes and split in 60k train and 10k test sets), we compute the centres for each class to determine the average image of every class $\{\boldsymbol{c}_i\}_{i=0}^{9}$. The label $\hat{\ell}_k$ of new instance $\boldsymbol{x}_k$ is defined as $\hat{\ell}_k = \arg\max_i \langle \boldsymbol{c}_i, \boldsymbol{x}_k\rangle^2$, *i.e.*, the centroid that looks most like $\boldsymbol{x}_k$. Thanks to the SPE, we can also estimate this quantity in the sketched domain:

$$\hat{\ell}_k^{\text{sk}} := \arg\max_i \tfrac{\kappa}{m} \langle \operatorname{sign}(\mathcal{B}(\boldsymbol{c}_i)), \mathcal{B}(\boldsymbol{x}_k)\rangle \tag{5}$$

Classification accuracy for different values of m over 500 trials, shows that $\hat{\ell}_k^{\text{sk}} \approx \hat{\ell}_k$ (see results table in $\% \pm$ std).

	Direct	$m = 200$	$m = 400$	$m = 800$	$m = 1600$
Accuracy [%]	81.2	69.3 ± 1.9	75.2 ± 1.25	78.6 ± 0.91	80.4 ± 0.79

6. Experiments II (with OPU) [2]

As the OPU operates on binary images, we first binarised our images (with a threshold set to maximise classification accuracy). In this experiment we restrict ourselves to the same dimension of the simulations in order to compare the two results.

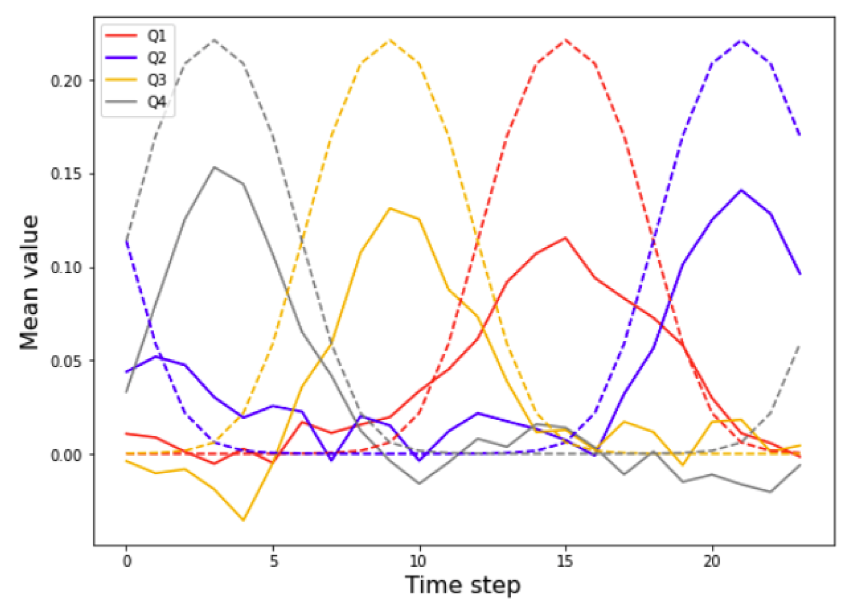

Figure 3: Estimation of quadrant occupancy functions per quadrant using the transformation of the OPU (ground truth in dashed).

Localised occupancy: We repeat the same experiment with the rotating disks, this time using the OPU to apply $\mathcal{B}$ in lieu of the artificially generated vectors. As shown in Fig. 3, the experiment shows that OPU process is capable of generating a result proportional to the ground truth.

Classification in the sketched domain: We also repeat the MNIST experiment using the to classify the hand-written digits of the MNIST dataset. Using the same number of features as in the simulated case, results are of lower accuracy (see results table in $\% \pm$ std):

	Direct	$m = 200$	$m = 400$	$m = 800$	$m = 1600$
Accuracy [%]	81.2	56.3 ± 0.84	64.9 ± 0.31	68.6 ± 0.6	70 ± 0.7

7. Conclusion & further research

- Further study the OPU to quantify differences with simulation
- Use quadratic sketching to detect anomalies in time series (videos for example), and demonstrate the possibility to localise it.

References

[1] R. Delogne, V. Schellekens, L. Jacques, *ROP Inception: Signal Estimation With Quadratic Random Sketching*, 2022, ESANN.

[2] A. Saade, et al., *Random projections through multiple optical scattering: Approximating kernels at the speed of light*, In IEEE ICASSP 2016 (pp. 6215-6219).

[3] Y. Chen, Y. Chi, A.J. Goldsmith, Exact and Stable Covariance Estimation From Quadratic Sampling via Convex Programming, IEEE Transactions on Information Theory, vol. 61, no. 7, 2015.